Available online at www.sciencedirect.com

ScienceDirect

Materials Today: Proceedings 5 (2018) 6208–6216

materialstoday: PROCEEDINGS

www.materialstoday.com/proceedings

ICMPC 2017

Effect of Air Entraining Admixture on Concrete under Temperature Changes in Freeze and Thaw Cycles

Amin Ziaei-Nia[a], Gholam-Reza Tadayonfar[a]*, Hamid Eskandari-Naddaf[a]

[a]*Department of Civil Engineering, Hakim Sabzevari University (HSU), Iran*

Abstract

The mechanism of air bubbles acting during freezing and thawing cycles considering various conditions has been studied by many researchers. On the other hand, simulation of the thermal stresses in concrete with finite element software is performed where the results have proved the capability of these methods. In this paper, stresses which are induced by temperature changes in the freezing and thawing cycles are investigated for non-air and air entrained concrete. Modelling procedures were implemented considering effects of aggregates, cement paste, and boundary conditions. The results have shown that air bubbles can play important role in uniform distribution of thermal stresses in concrete which may lead to decreased maximum stress that occurs in concrete. It can also cause the plastic strains in the interfacial transition zone (ITZ) to be controlled.

*Keywords:*Freeze and Thaw, Finite Element, Air Entrained, Durability, Concrete ;

1. Introduction

The most important aspect of concrete durability in areas exposed to cold regions conditions is its resistance against freeze and thaw cycles. This damage starts with concrete surface scaling and continues into the concrete depth[1]. One of the most effective parameters in increasing concrete durability in these conditions is applying air entraining admixture (AEA) in concrete mixture which provides different effects on mechanical properties of concrete [2]. For the first time in the mid-1930s, researchers found the effect of air bubbles in the concrete durability. This discovery can be mentioned as a revolution in concrete applications[3, 4]. A distinction are made between deliberately entrained air bubbles which are small and are distributed uniformly through the cement paste

* Gholam-Reza Tadayonfar. Tel.: +985144012771; fax: +985144012773.
*E-mail address:*r.tadayon@hsu.ac.ir

and accidentally entrapped air bubbles with random size and shaping which the concrete durability is significantly affected with the deliberately entrained one[5, 6].Stresses have arisen in concrete as a result of freezing and thawing cycle is dependent on several factors one of which is temperature changes. The tension amounts are dependent on the coefficient of thermal expansion of aggregates and cement paste[7].

The expansion of the cement paste is often greater than the thermal expansion of aggregate. This factor for cement paste, depending on the moisture content is changed from 11×10^{-6} ºC^{-1} to 16×10^{-6} ºC^{-1}. This factor for stone materials which produced from natural stones is often in the range of 5×10^{-6} ºC^{-1} and 13×10^{-6} ºC^{-1}. If the difference between the thermal expansion coefficient of cement paste and aggregate is more than 5.5×10^{-6} ºC^{-1} , the concrete durability in the freezing and thawing cycle is strongly affected [8]. An experimental study for analyzing the effects of temperature changes between room temperature and100 ºC on deflections of cement paste and mortar beams under load were done previously. The results showed that heating the beam after load application make the cement paste and mortar beams deflect excessively where deflections rarely lead to failure at low stresses and after moderate heating[9]. The results of studies on the tensions induced by daily thermal changes of pavements yielded that these stresses can be effective in concrete damages which the effects may be considered as a fatigue load on concrete pavements which gradually reduces the concrete lifetime [10].

To achieve a good understanding of the temperature distribution of and thermal stresses occurring in concrete, finite element method can be very efficient to operate. Nowadays, applying finite element software in modeling of thermal stresses in concrete are developing widely. Modeling of thermal stresses at high temperatures [11], massive concrete structures [12, 13], and structures exposed to fire [14] has shown acceptable results. Tensions caused by changes in temperature of environment in the concrete pavement was also the noticeable issue of some researches [15]. Modeling structures during the service life, under the influence of thermal stresses caused by climatic factors were also considered by some researchers [16-19].

Understanding the transport of water and associated electrolytes in concrete including permeability, kinetics of water and air movement within cement and concrete, and resistance to freezing and thawing cycles have not been done considerably. Thus it may be significant to develop sufficient meso-scale models and connect them to macroscopic properties such as resilience and permeability. To this end, researchers are investigating a two-dimensional meso-scale model of concrete to better understand the mechanism of damage in freezing and thawing conditions [20]. Moreover, Lopez et al.[21] have modelled fresh concrete with and without AEA under the influence of heat of hydration and surface heat flux. The goal of this work is thus to develop the presented model of [22] for hardened concrete in order to realize the role of air bubbles in restraining the tensions which are only caused by temperature changes in freeze and thaw cycles of concrete.

2. Finite Element Model

2.1. General descriptions

A number of concrete representative volume elements (RVE) were proposed using various sizes and numbers of air bubbles. Applying an RVE reduces the analyzing time for models containing air voids, rather than having to investigate the effects of the voids by using a homogeneous model. Since the modeling should be done precisely and also for considering concrete sample in the actual environment, two types of supports were applied in the model. The

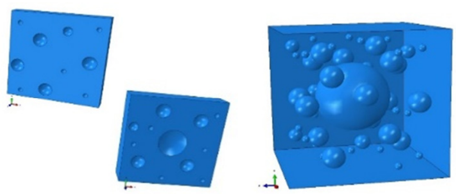

Fig.1. The distribution and kind of air bubble modelling in air entrained concrete.

presented model was also verified with the experimental results of Lopez et al. [21] in which size and number of air bubbles specified for each RVE for concrete sample with 10% AEA. The distribution and kind of air bubble modelling is shown in the Fig.1.

2.2. Material modelling of concrete

The behavior of concrete has been investigated in the elastic mode. In addition, the behavior of concrete, cement paste, and aggregate were analyzed in the plastic mode using concrete damaged plasticity property. Concrete damaged plasticity model implemented in ABAQUS[22] is used herein due to the this fact that other models like smeared cracking model usually encounters numerical difficulties on analysis under cyclic load.

2.3. Boundary conditions and loading

Two types of boundary conditions for RVEs considered include:
- None of the RVE is constrained.
- Two sides of RVE are constrained in direction of the Z axis.

Also there is no load on the model and the forces yielded in RVEs are only caused by temperature changes. In order to simulate freeze and thaw test, the RVE temperature changed from 20 ºC to -20 ºC in 12 hours and changed inversely from-20 ºC to 20 ºC in the next 12 hours. This process was repeated over 20 cycles for each RVE.

2.4. The selection of element type and meshing

Because of the spherical shape and distribution type of air bubbles in the concrete, the model should be constructed in three-dimensional state. The applied meshes are pyramid with four node (C3D4). This element in comparison with the high-order isoparametric element, although the accuracy of this element is slightly lower, can reduce to a lot of freedom degree, which can greatly reduce the computational cost. Fig. 2 shows type of meshes in the non-air and air entrained concrete.

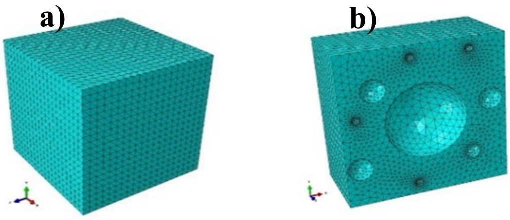

Fig. 2. Quality of RVE meshing for (a) non-air and (b) air entrained concrete.

3. Validity of FEM Modelling

In the report of Lopez et al. [21] the results of experimental tests have shown good compatibility with the FEM results. Fig.3 shows steps of modeling and meshing of air entrained concrete sample presented by Lopez et al. [22].

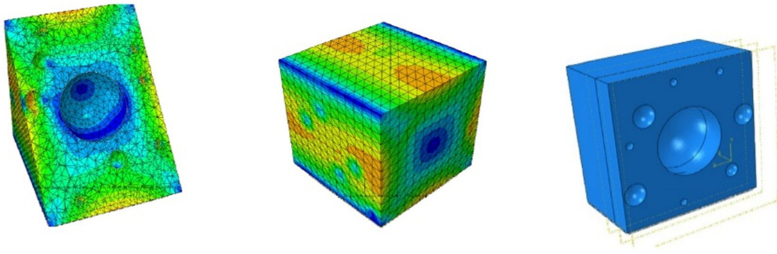

Fig. 3. Finite element model and mesh of air entrained concrete sample in study of Lopez al. [21]

Modeling process including the type and size of meshes, size, number and distribution of air bubbles and dimensions of RVEs, was performed based on the information provided in this report [22].

The RVEs are described below[21]:

- RVE1: 2-mm cube of non-air entrained concrete, used for comparison to air entrained concrete.
- RVE2: 2-mm cube of concrete with 10 percent air content, the air void size distribution is: one 1 mm, eighteen 0.3 mm, six 0.2 mm, and twenty-four 0.1 mm

Compared results of the presented model of this study with the observations reported by some researchers for concrete that is exposed to atmospheric factors, showed good accuracy of the model which will be discussed in the next part.

4. Results and Analysis

In Fig. 4 the maximum principal stresses for RVE of non-air entrained concrete are showed in which none of the element sides is constrained. Although the stress values are not distributed uniformly, it can be seen that in most part of the RVE the stresses are very low with the approximate value of 10-13 MPa. The stress values are so low as it may not reach to the stress values even near the maximum and plastic range of concrete. In Fig. 5, the stress in direction of the Z axis and at different distances from the middle section are shown. As can be seen, the stress values are also very small.

stresses caused by temperature changes and the stress contours in direction of the Z axis at different distances from the middle section for air entrained concrete are shown in Figs. 6 and 7 respectively. It is so obvious in these two figures, the stress values are also so small and near 10-14 MPa. By comparing the stresses in Figs. 4 and 5 with the Figs. 6 and 7, it can be seen although these stresses are very small, but the use of AEA about 10 % make the stresses to be about 10 times lower.

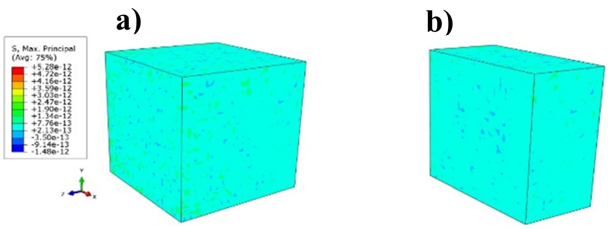

Fig. 4. The maximum principal stresses in non-air entrained concrete. (a) overview and (b) middle section of the RVE

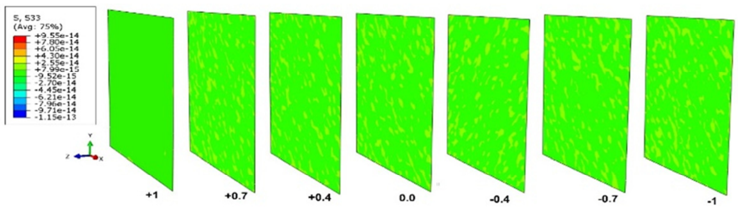

Fig.5. Stress contours of non-air entrained concrete in direction of the Z axis and at different distances (mm) from the middle section

Fig. 5 also mentioned that the stresses are distributed around the air bubbles which may lead to more uniform distribution of stresses caused by temperature changes in the freeze and thaw conditions. It was also observed that the smaller bubbles play more active role in absorbing the stresses around their selves which result in more uniform distribution of the stresses. This, leads to reduce the maximum stress applied to concrete by a constant amount of load (thermal load). Therefore, the concrete sample is expected to contribute relatively more yield stress.

Observations of researchers also confirms that the air bubbles which are smaller and also closer to each other can be more effective in increasing the concrete durability[5, 6]. Moreover, the results have proved that continues increasing in the specific surface of the air bubbles can affect significantly on the application of AEA for raising the concrete durability [23]. Although a free to move concrete element will have no stress, movements of concrete samples, inducing thermal stresses normally due to temperature variations can be always considered restrained. When concrete is placed against rigid material, like adjacent older concrete element, the structure is constrained from moving and strains associated with temperature changes cannot occur [24].

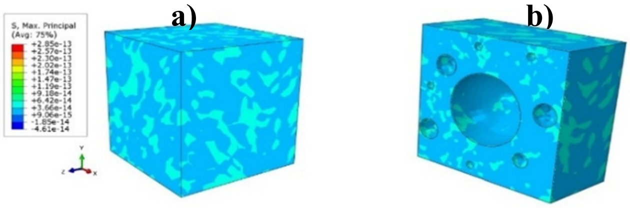

Fig. 6. The maximum principal stresses in air entrained concrete. (a) overview and (b) middle section of the RVE

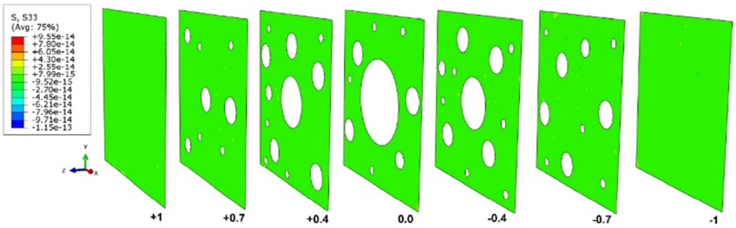

Fig.7. Stress contours of air entrained concrete in direction of the Z axis and at different distances (mm) from the middle section

When a concrete sample is exposed to harsh environmental conditions, some of its sides are somewhat constrained due to the various situations. For example, in the issue of pre-cast concrete kerbs the sides which are in contact with each other in two kerbs, are somewhat constrained. In order to investigate the mentioned conditions and to better understand the amount of maximum applied stresses to concrete sample, the RVE model is proposed in both states of with and without air bubbles considering elastic properties with constrained boundary condition which are applied to the two sides of sample in direction of the Z axis. The results indicate that the maximum principal stresses for non-air entrained concrete contain huge values so that in a wide range of middle section of RVE (Fig. 8 (a)) the stress values are close to 17 MPa where the minimum stress is about 5.4 MPa. As seen, the obtained stress values are noticeably more than the unconstrained boundary condition and may cause concrete deterioration in many cases.

While it can hardly be said that a concrete sample, in the reality, is constrained completely, comparison of the results between Figs. 4 with 8 and Figs. 6 with 9 show that the boundary conditions can be a very important parameter in determination of thermal variations induced stresses.

Despite applying AEA in concrete sample, the stress values provide large numbers (Fig. 9). Furthermore, the maximum and minimum stress values are decreased respectively from 148 and 5.5 MPa to 85 and 1.8 MPa for non-air and air entrained concrete respectively. Using AEA is thus so effective in decreasing the stress values to be in a durable limitation of the concrete sample. It is so obvious in Fig. 9 that the air bubbles absorb the stresses which helps the distribution of the stress values in concrete sample to be more uniform. This, may then reduce the differences between the stress values of external surface and central core of concrete.

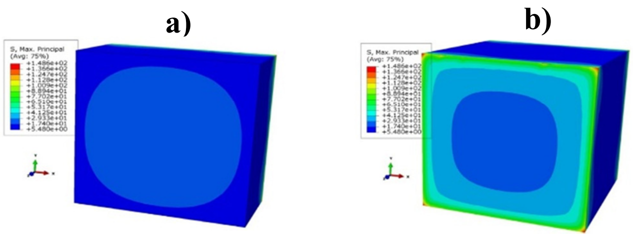

Fig.8. The maximum principal stresses in non-air entrained concrete with two constrained sides in direction of Z axis. (a) The middle section and (b) overview of the RVE in elastic state.

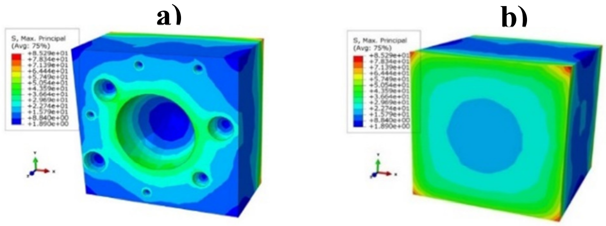

Fig.9. The maximum principal stresses in air entrained concrete with two constrained sides in direction of Z axis. (a) The middle section and (b) overview of the RVE in elastic state.

Concrete as a heterogeneous mixture involves some differences in thermal properties of aggregates and cement paste. The more the differences, the more decreased durability of concrete in harsh climatic conditions [25]. Considering this fact may help to better understanding the concrete operation in freeze and thaw cycles. In this regard, the concrete model was proposed due to various properties of both concrete and cement paste where the results are represented in Figs. 10 to 13. In order to make the modeling process easier, shape of aggregates considered cubic with the same setting places in whole models.

The overview of maximum principal stresses in the middle section of RVE are presented in Fig. 10. The stresses contour of cut RVE sections is shown in Fig. 11 by considering various properties of aggregate and cement with different distance from the middle section. As seen, large amount of differences for stresses are obtained in comparison with the state that the concrete was presented as a

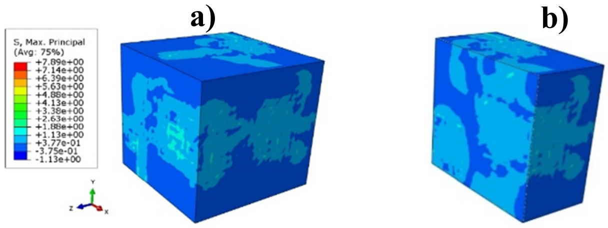

Fig.10. The maximum principal stresses in non-air entrained concrete considering properties of aggregates and cement paste separately. (a) overview and (b) the middle section of the RVE.

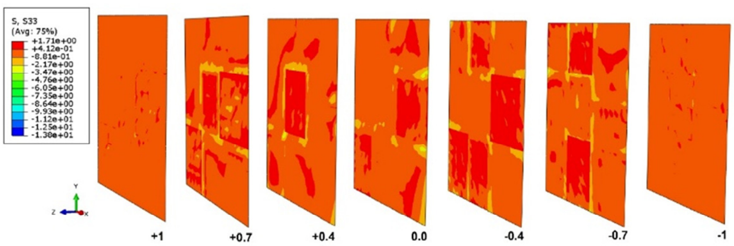

Fig.11. Stress contours of non-air entrained concrete considering properties of aggregates and cement paste separately in the direction of the Z axis and at different distances (mm) from the middle section.

homogeneous material (Figs. 4 and 5). Due to this fact, it is so clear that the various thermal properties of aggregates and cement paste should be considered especially in situations where the concrete thermal stresses are important.

The maximum principal stress values and stress contours of non-air entrained are represented respectively in Figs. 12 and 13 considering properties of aggregates and cement paste in the direction of the Z axis and at different distances from the middle section. As seen in the Figs. 10 and 12, the maximum stress values occur in the interfacial transition zone (ITZ) between the cement paste and aggregates.

Although these stresses have to be reduced in air-entrained concrete, but it still provides a noticeable rate. Likewise, comparing these two figures clearly illustrates the kind of uniform distribution of air bubbles in the RVE. This trend

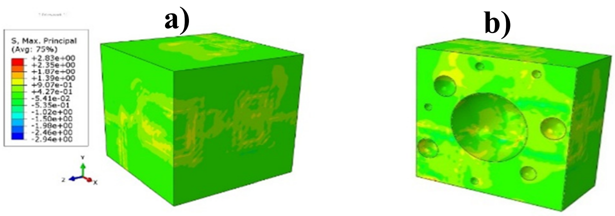

Fig.12. The maximum principal stresses in air entrained concrete considering properties of aggregates and cement paste separately. (a) overview and (b) the middle section of the RVE.

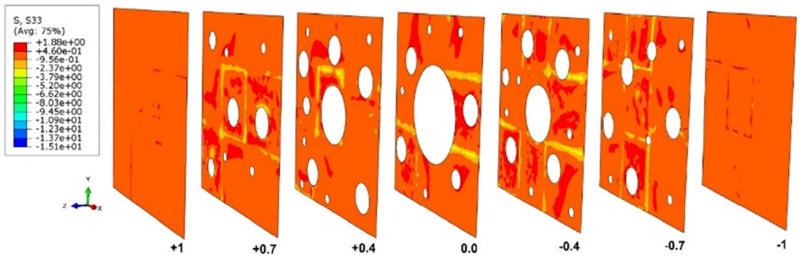

Fig.13. Stress contours of air entrained concrete considering properties of aggregates and cement paste separately in the direction of the Z axis and at different distances (mm) from the middle section.

can also be seen by comparing Fig. 11 and 13 so that it is obvious that the stress values in aggregates are more than cement paste. Meanwhile, from Fig. 13 which related to air-entrained concrete it can be realized that the stress distribution in aggregates and cement paste are almost identical. Moreover, such different stresses between ITZ and aggregates will produce micro-cracks [26], causing plastic strains in the ITZ and finally decreased concrete durability (Fig.11).

Contours for plastic strain magnitude (PEMAG) for both non-air entrained and air entrained concretes are shown in Fig. 14 where the effect of air bubbles in decreasing the ITZ areas with plastic strains is so obvious. Since the ITZ is the weakest area in the concrete, it should be considered as a most effective parameter in determination of concrete properties specifically its durability [6]. Form Fig. 14 it can be concluded that temperature variations have the most effects on ITZ in freeze and thaw cycles. Applying AEA is thus an appropriate approach in reducing the thermal damages of concrete.

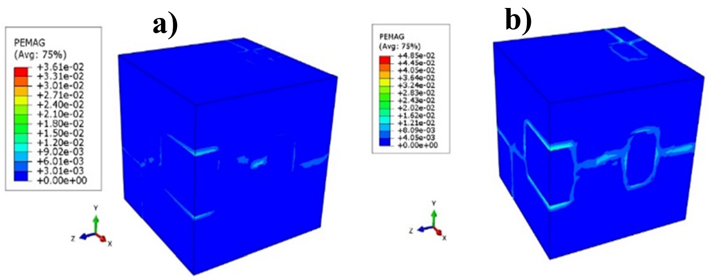

Fig. 14. plastic strain magnitude for (a) air entrained and (b) non-air entrained concrete.

The average stress values of aggregates during freeze and thaw cycles for both non-air and air entrained concretes have been depicted in Fig. 15. As seen, the maximum and minimum stress values in air-entrained concrete in each cycle is noticeably lower than non-air entrained concrete which emphasized again the influence of air bubbles in reducing the internal stresses caused by temperature variations resulting in increasing the concrete durability. The more the cycles, the more stress reduction so that this value for non-air entrained concrete is less that air-entrained concrete. Increasing the freeze and thaw cycles may cause the more parts of RVE to be in plastic area. Since the ITZ is mentioned as the weakest part of concrete, it behaved plastic as the first part of concrete which causes less distributed stress values between aggregates and cement paste.

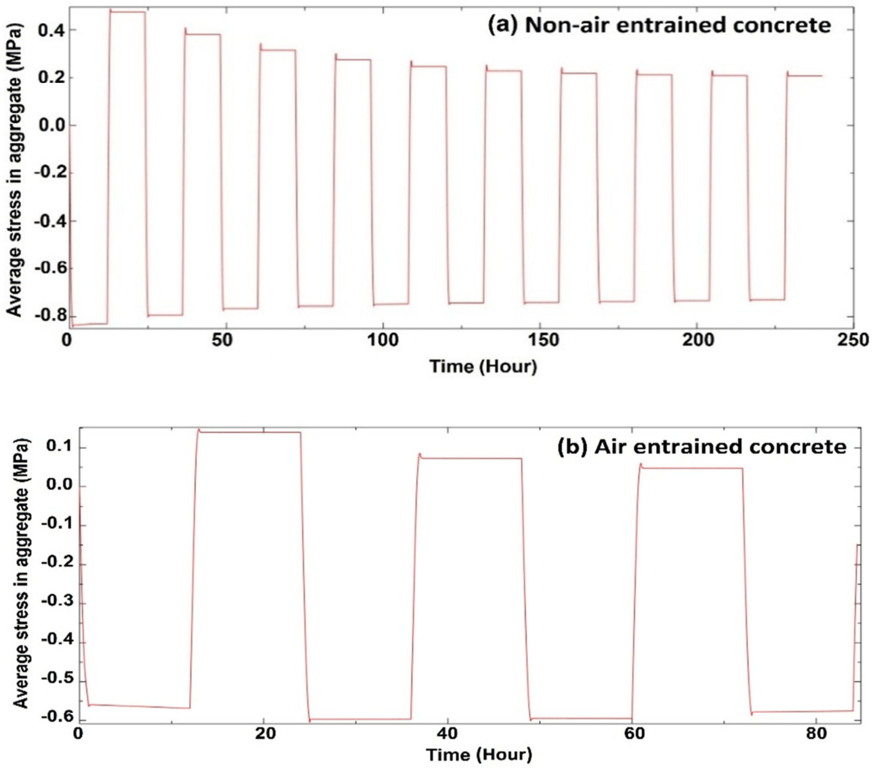

Fig. 15. Average occurred stress values in aggregates vs. time for (a) non-air and (b) air entrained concrete.

Results of previous researches have mentioned that thermal stresses may not cause concrete deterioration until their values are less than concrete tensile capacity [6]. The results of this study can show that the thermal stresses occurred in the investigated concrete samples are less than the tensile stresses of normal concretes (Figs 10-13). However, it should be considered that the tensile stress capacity of ITZ is much less than normal concrete [6]. On the other hand, applying cyclic loads to concrete cause concrete to be deteriorated in a much less values than normal conditions [9]. Therefore, regardless of other suggested mechanisms for effects of AEA on increasing concrete durability, it can be mentioned that freeze and thaw cycles in normal (non-air entrained) conditions can cause concrete to be damaged due to relatively large differences between the aggregates and cement paste stresses and ITZ ones. As regard, Al-Tayyib et al. [25] found that the concrete structures subjected to temperature variations in a range between 20 to 80oC, experience significant quality deterioration so that their permeability becomes 4 to 6 times greater after 90 heating and cooling cycles. This, leads to more convenience water penetration through concrete sample and then increased water volume during freezing, resulting in early concrete deterioration. However, air bubbles significantly reduced the probability of ITZ deterioration by uniform distribution and reducing the stresses values, causing increased concrete durability.

5. Summary and Concluding Remarks

- Finite element modelling of concrete behaviour under effects of thermal stresses would be so useful if the differences between thermal properties of aggregates and cement paste is considered.
- Applying air bubbles in concrete mixture causes the thermal stresses to be distributed more uniformly in which the smaller sized bubbles are more effective. Typically, it can also be mentioned that the AEA may intensively reduce the maximum thermal stress values.
- The differences between the aggregates and cement paste stresses and ITZ ones can be sufficiently reduced using AEA which followed by later deterioration and more durability of concrete.
- Boundary condition and also its placement can play a very important role in determination of stresses which induced by freezing and thawing cycles.
- The lower values of differences between thermal properties of aggregates and cement paste leads to reduced thermal stresses applied to concrete sample.

References

[1] H. Shang, Y. Song, J. Ou, Behavior of air-entrained concrete after freeze-thaw cycles, Acta Mechanica Solida Sinica 22(3) (2009) 261-266.
[2] ACI, 201.2R-08, Guide to Durable Concrete. ACI manual of concrete practice, American Concrete Institut, Farmington Hills 2008.
[3] L. Du, K.J. Folliard, Mechanisms of air entrainment in concrete, Cement and concrete research 35(8) (2005) 1463-1471.
[4] A.F. E, Air entraiend concrete, Research Laboratory Testing and Research Division, 1944.
[5] J. Elsen, N. Lens, J. Vyncke, T. Aarre, D. Quenard, V. Smolej, Quality assurance and quality control of air entrained concrete, Cement and concrete research 24(7) (1994) 1267-1276.
[6] A.M. Neville, Properties of concrete, 5th Edition ed.2012.
[7] Z.P. Bazant, G. Cusatis, L. Cedolin, Temperature effect on concrete creep modeled by microprestress-solidification theory, Journal of Engineering Mechanics 130(6) (2004) 691-699.
[8] A.M. Neville, J.J. Brooks, Concrete technology, 1987.
[9] T.C. Hansen, L. Eriksson, Temperature change effect on behavior of cement paste, mortar, and concrete under load, JOURNAL OF THE AMERICAN CONCRETE INSTITUTE1966.
[10] K.-m. NIU, B. TIAN, Equivalent fatigue thermal stress coefficient of cement concrete pavement [J], China Journal of Highway and Transport 5 (2006) 005.
[11] C.J. Robson, Modelling the transient strain behaviour of concrete exposed to elevated temperatures, (2012).
[12] G. De Schutter, Finite element simulation of thermal cracking in massive hardening concrete elements using degree of hydration based material laws, Computers & Structures 80(27) (2002) 2035-2042.
[13] Z. Bofang, Thermal stresses and temperature control of mass concrete, Butterworth-Heinemann2013.
[14] W. Gao, J.-G. Dai, J. Teng, G. Chen, Finite element modeling of reinforced concrete beams exposed to fire, Engineering structures 52 (2013) 488-501.
[15] J.-H. Jeong, D.G. Zollinger, J.-S. Lim, J.-Y. Park, Age and moisture effects on thermal expansion of concrete pavement slabs, Journal of Materials in Civil Engineering 24(1) (2012) 8-15.
[16] A. Saetta, R. Scotta, R. Vitaliani, Stress analysis of concrete structures subjected to variable thermal loads, Journal of Structural Engineering 121(3) (1995) 446-457.
[17] F. Sheibany, M. Ghaemian, Effects of environmental action on thermal stress analysis of Karaj concrete arch dam, Journal of engineering mechanics 132(5) (2006) 532-544.
[18] H. Mirzabozorg, M. Hariri-Ardebili, M. Shirkhan, S. Seyed-Kolbadi, Mathematical modeling and numerical analysis of thermal distribution in arch dams considering solar radiation effect, The Scientific World Journal 2014 (2014).
[19] D. Santillán, E. Salete, M. Toledo, A new 1D analytical model for computing the thermal field of concrete dams due to the environmental actions, Applied Thermal Engineering 85 (2015) 160-171.
[20] T. Zhou, M.Z. Bazant, R.J.M. Pellenq, Modeling freeze-thaw in concrete, CSHub@MIT, Research Brief (5) (2015).
[21] M. Lopez de Murphy, C. Lissenden, C. Xiao, Technology Evaluation on Characterization of the Air Void System in Concrete, 2009.
[22] D. Systèmes, Abaqus analysis user's manual, Simulia Corp. Providence, RI, USA Volume III: Materials (2013).
[23] Pca, Control of Air Content in Concrete, Concrete Technology Today Volume 19/Number 1 (April 1998).
[24] M.N. Amin, J.-S. Kim, Y. Lee, J.-K. Kim, Simulation of the thermal stress in mass concrete using a thermal stress measuring device, Cement and Concrete Research 39(3) (2009) 154-164.
[25] A. Al-Tayyib, M. Baluch, A.-F.M. Sharif, M. Mahamud, The effect of thermal cycling on the durability of concrete made from local materials in the Arabian Gulf countries, Cement and Concrete Research 19(1) (1989) 131-142.
[26] Q. Ma, R. Guo, Z. Zhao, Z. Lin, K. He, Mechanical properties of concrete at high temperature—A review, Construction and Building Materials 93 (2015) 371-383.